The Astrophysical Journal, 609:L95–L98, 2004 July 10
© 2004. The American Astronomical Society. All rights reserved. Printed in U.S.A.

CHROMOSPHERIC OSCILLATIONS IN AN EQUATORIAL CORONAL HOLE

Scott W. McIntosh
Universities Space Research Association, Cooperative Program in Space Science, 7501 Forbes Boulevard, Suite 206, Seabrook, MD 20706; and Laboratory for Astronomy and Solar Physics, NASA Goddard Space Flight Center, Mail Code 682.3, Greenbelt, MD 20771; scott@grace.nascom.nasa.gov
Bernhard Fleck
European Space Agency, Research and Scientific Support Department, NASA Goddard Space Flight Center, Mail Code 682.3, Greenbelt, MD 20771; bfleck@esa.nascom.nasa.gov
and
Theodore D. Tarbell
Lockheed Martin, Solar and Astrophysics Laboratory, 3251 Hanover Street, L9/41, Building 252, Palo Alto, CA 94304; tarbell@lmsal.com
Received 2004 March 12; accepted 2004 May 25; published 2004 June 8

ABSTRACT

We report phase-difference and travel-time analyses of propagating chromospheric oscillations in and around an equatorial coronal hole as observed by *TRACE*. Our results suggest a significant change in atmospheric conditions at the base of the chromosphere inside the coronal hole relative to its boundary and quiet-Sun regions.

Subject headings: Sun: atmospheric motions — Sun: chromosphere

1. INTRODUCTION

Coronal holes are the lowest density plasma components of the Sun's outer atmosphere. They are associated with rapidly expanding magnetic fields and a multitude of wave phenomena and are an apparent source of the fast solar wind (see the recent review of Cranmer 2002). The low plasma density in coronal holes and dark signature in coronal extreme-ultraviolet (EUV) images would imply that the stratification of the plasma inside the coronal hole is significantly different from that outside of it. Likewise, the magnetic field topology in and around any coronal hole is a delicate, but pervasive, balance of a largely "open" field that is surrounded by "closed" field structures on many spatial scales.

Recent investigations of chromospheric oscillations observed by the *Transition Region and Coronal Explorer* (*TRACE*; Handy et al. 1999) and the *Solar and Heliospheric Observatory* (*SOHO*; Fleck et al. 1995) have demonstrated that the structure and strength of the underlying magnetic field significantly alter and inhibit the observed wave fields (e.g., McIntosh et al. 2001, 2003; McIntosh & Judge 2001; McIntosh & Smillie 2004). We therefore expect that a coronal hole presents a topologically obvious place to study chromospheric oscillations at the interface between open and closed regions of the solar atmosphere.

In the following section we present *TRACE* observations of chromospheric oscillations in an equatorial coronal hole region. In § 3, we discuss their analysis and the implications of the derived diagnostics on the chromospheric plasma topography just above the temperature minimum at the root of the solar wind.

2. DATA AND ANALYSIS

We present *TRACE* time series data in the 1700 and 1600 Å ultraviolet (UV) continua bandpasses with a 12 s cadence observed 2003 July 14 commencing at 00:09 UT (and ending at 01:19 UT). We note that the *TRACE* bandpass observations are not simultaneous, the 1700 Å image being taken 4 s before the 1600 Å image, but this is accounted for in the presented analysis. Our need to consistently analyze the same spatial region across the bandpasses at full *TRACE* spatial resolution (0.5 arcsec^2) means that the time series data for each bandpass must have the effects of solar rotation removed and be carefully co-aligned. To this end we employ the *TRACE* IDL routine "tr_get_disp_2d.pro" image correlation procedure that is discussed in Krijger et al. (2001) and McIntosh et al. (2003). Context for the *TRACE* observations is provided by the *SOHO* EUV Imaging Telescope (EIT; Delaboudiniere et al. 1995) 195 Å image taken at 00:08 UT that appears in Figure 1. The *TRACE* field of view (FOV) is shown as the thick red rectangular region, while the yellow and orange contours represent the 100 and 200 data number (DN) intensity levels of the EIT image, respectively. These contour levels qualitatively designate the coronal hole boundary.

In Figure 2 we show the 1700–1600 Å phase-difference gradient ($M_{\Delta\phi}$; McIntosh et al. 2003; Fleck & McIntosh 2003) map for the 2003 July 14 data set. Also shown in this figure are the corresponding locations of the EIT 100 and 200 DN intensity levels (again, as the thick yellow and orange contours) and the black (negative) and white (positive) closed contours of the *SOHO* Michelson Doppler Imager (MDI; Scherrer et al. 1995) longitudinal magnetic field ($B_\parallel$) magnitude of 20 G. Clearly, inside the coronal hole the $M_{\Delta\phi}$ map shows consistently large values that can be compared to the (very) quiet-Sun example presented in Figure 6*b* of McIntosh et al. (2003). Likewise, there is a large contrast between the interior ($\langle M_{\Delta\phi}\rangle \sim 5^\circ$ mHz^{-1}) and boundary regions ($\langle M_{\Delta\phi}\rangle \sim 1^\circ$ mHz^{-1}) of the coronal hole. Unfortunately, as discussed in § 3 of McIntosh et al. (2003), $M_{\Delta\phi}$ ($\approx \Delta z/V_{\rm phase}$) is not a unique measure; being a mixture of the vertical separation (Δz) of the two bandpasses and the phase velocity ($V_{\rm phase}$) of the waves modes traveling between them. Therefore, the ambiguous interpretation of Figure 2 is that in the interior of the coronal hole, either we have a larger Δz or the phase velocity of the wave modes is lower.

As a more intuitive, but no less ambiguous, alternative to $M_{\Delta\phi}$ we introduce a "travel-time" diagnostic between the two bandpasses (see, e.g., Jefferies et al. 1994, 1997; Jefferies 1998). The travel time (Δt) at any particular frequency (ν) can be computed at the highest possible spatial resolution[1] by taking the time series in each bandpass and taking a Gaussian filter, $G(\nu;\ \delta\nu)$, about ν with a relatively narrow $1/e$ width ($\delta\nu$). Using

[1] Travel-time estimation does not need the multipixel binning that is required to accurately compute the noise-susceptible $M_{\Delta\phi}$ as discussed in Fleck & McIntosh (2003).

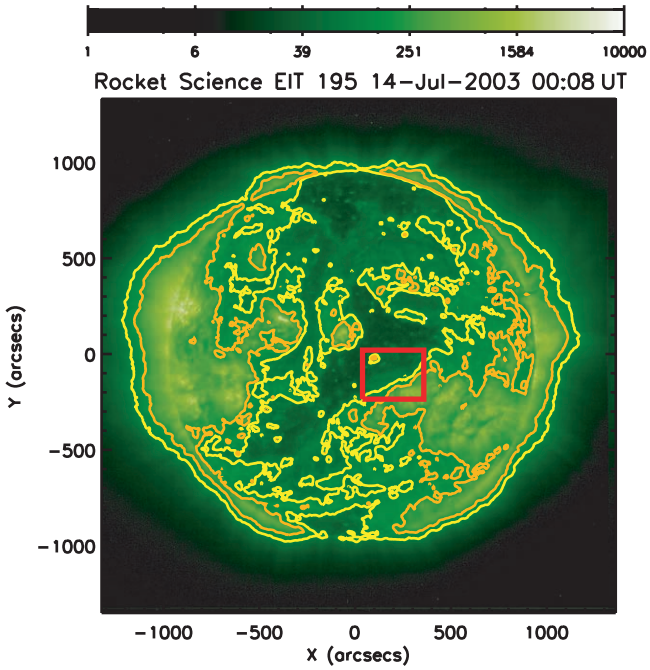

FIG. 1.—*SOHO* EIT 195 Å context image from 2003 July 14, 00:08 UT. The red rectangular region shows the *TRACE* FOV, while the yellow and orange contours show the 100 and 200 DN intensity levels in the image, respectively.

the filtered time series in each bandpass we construct the signal cross-correlation as a function of the lag time between the time series pairs over a (ν-dependent) number of exposures; say 10 (120 s) for a filter frequency of 7 mHz. By fitting a quadratic curve to the maximum of the resulting cross-correlation function, we are able to achieve subexposure values of the lag time. A negative lag time, as is the common convention, indicates that the signal in the 1700 Å bandpass leads that in 1600 Å by that amount of time. Hereafter, we equate this lag time to the oscillation travel time,[2] and a negative value is indicative of an upward disturbance.

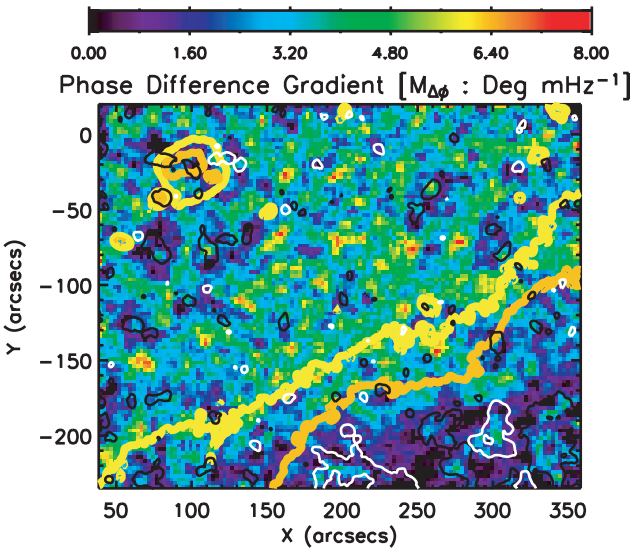

FIG. 2.—Phase-difference gradient map at 5 × 5 *TRACE* pixel resolution. The black and white contours, respectively, indicate 20 G levels of negative and positive *SOHO* MDI longitudinal magnetic field strength, respectively. The thick yellow and orange contours show the 100 and 200 DN intensity levels in the image, as shown in Fig. 1.

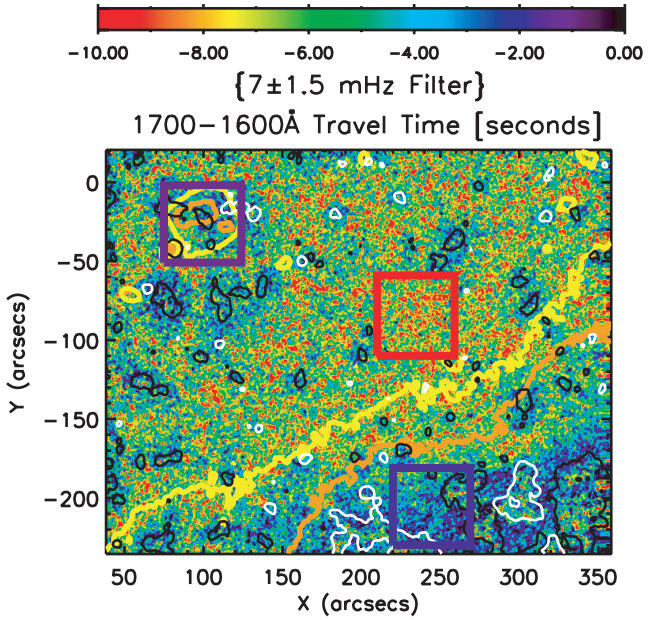

FIG. 3.—Travel-time map at full *TRACE* resolution. The contours on the figure are the same as in Fig. 2. The colored rectangles are used to denote regions of coronal hole interior (*red*), coronal hole boundary/exterior (*blue*), and coronal hole arcade (*purple*).

In Figure 3 we show the travel-time map, at full *TRACE* resolution, for the coronal hole region where the color scale now indicates the travel time of the disturbance. Clearly, there is a notable difference in the time-travel map between the coronal hole interior and exterior. In an effort to quantify this difference, we have placed three 50″ × 50″ regions in the figure: one in the coronal hole interior (*red*), another in the coronal hole boundary/exterior (*blue*), and a third over the EUV arcade visible in the 195 Å EIT image (*purple*).

In Figure 4 we sample across the 11 filters spanning the frequency space (3–15 mHz) in each of the three regions shown

[2] Incidentally, it is trivial to show that the travel time is equivalent to the phase difference between the two signals at that frequency; $\Delta\phi \sim 2\pi\Delta t/\nu$.

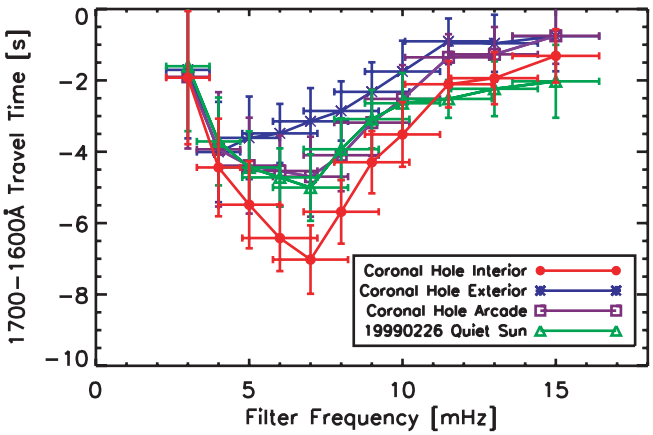

FIG. 4.—Region averaged travel times as a function of frequency corresponding to the colored regions in Fig. 3 and those from the quiet 1999 February 26 data (*green curve*).

in Figure 3 plus the average of three regions in the well-studied (very) quiet-Sun 1999 February 26 *TRACE* data set (*green curve*; McIntosh & Judge 2001; McIntosh et al. 2003). Each colored curve is comprised of the region mean Δt, with vertical error bars indicating the standard deviation of Δt in the region and horizontal error bars indicating the $1/e$ width of the Gaussian filter. While the four curves match (within the errors) at low and high frequencies, there is significant departure in travel time between the red curve and the others between 5 and 10 mHz, with the most obvious difference being between the red and blue curves, the coronal hole interior, and the exterior, respectively. The overturn in all of the curves beyond 8 mHz, as also reported in Krijger et al. (2001) and Fleck & McIntosh (2003), suggests that the high-frequency region of the spectrum is noisy and suffers from artifacts, as the travel time should flatten out and be constant for sound waves significantly above the acoustic cutoff frequency (e.g., Deubner & Fleck 1990).

The preceding discussion largely neglects the influence of the photospheric magnetic field on the chromospheric oscillations. In an effort to address this, we follow the method provided in § 2 of McIntosh et al. (2003) and construct the plasma-β transition height (βTH) map in the *TRACE* FOV. We do so by extrapolating the co-aligned MDI $B_{\parallel}$ and computing the magnetic pressure ($||\boldsymbol{B}||^2/8\pi$). We employ a standard model atmosphere (e.g., model C of Vernazza et al. 1981) to provide a gas pressure, and βTH is simply the height in the atmospheric cube where the ratio of the gas and magnetic pressures, the plasma-β, is of the order of unity. For this particular example, the βTH map is shown in Figure 5. Drawing comparison between Figures 3 and 5, we can see that there is a strong correspondence between the general features of both the βTH and the Δt maps (cf. Fig. 7 of McIntosh et al. 2003), but in particular the regions of high βTH and the longest travel times at 7 mHz.

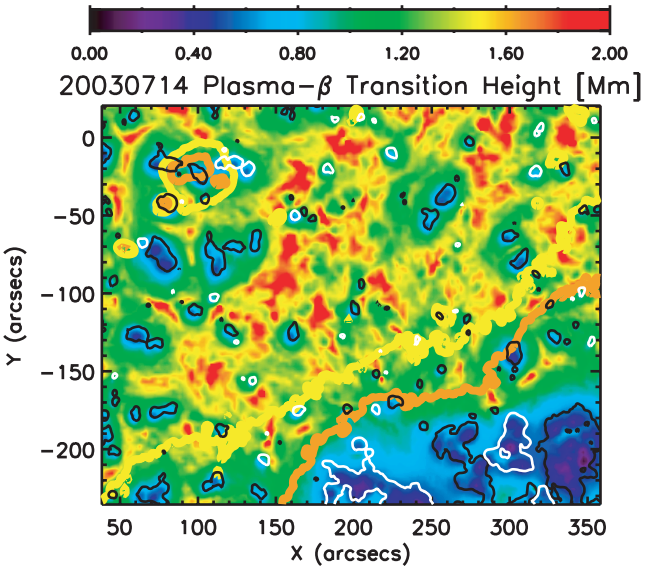

FIG. 5.—Spatial variation in the altitudes at which the extrapolated plasma-β is of the order of unity in the *TRACE* FOV, the βTH (cf. McIntosh et al. 2003). The contours on the figure are the same as in Fig. 2.

3. DISCUSSION

It is not a stretch to say that large travel times in the coronal hole interior are simply an extension of the internetwork regions shown in McIntosh et al. (2003), where the magnetic field is now weaker and largely unipolar. It would appear that the polarity distribution and mixing play an important role in allowing an observer to distinguish a coronal hole from quiet-Sun plasma.

As a result of the weak and largely unipolar magnetic field in the coronal hole interior, βTH is very high ($\geq$1 Mm; cf. Fig. 5), in fact, significantly higher than the formation heights of the *TRACE* UV continua observed (400–500 km; Judge et al. 2001). This is also the case in the internetwork regions of the very quiet Sun (see, e.g., Fig. 6 of McIntosh et al. 2003). In a zeroth-order approximation to the phase velocity, the waves that we are observing can therefore be interpreted as being predominantly acoustic in nature with little magnetic modification of their phase speed. Making this assumption, the observed travel time, $\Delta t \approx \Delta z/V_s$, is directly proportional to the height difference between the two bandpasses, where V_s is the local sound speed in the lower chromosphere (~6 km s^{-1}). For a filter frequency of 7 mHz, therefore, the 4 s difference between the red and blue curves in Figure 4 can be approximated by a difference in Δz of 24 km between the the coronal hole interior and its boundary. The green and purple curves effectively match across all frequencies within the errors, which is most likely associated with the presence of mixed polarity magnetic fields and the inclusion of a higher density of closed topological structures in those regions; certainly that is the perception of typical quiet-Sun regions. The difference between the red and green curves is of particular interest. Again, under the assumption that sound waves propagate at these heights in the chromosphere, it demonstrates that the mean difference of Δz between that of the coronal hole interior and that of the very quiet Sun[3] is of the order of 12 km (on a pixel-to-pixel basis it is larger: ≈24 km), a not insignificant fraction of a scale height near the chromospheric temperature minimum (~100 km). This indicates a substantial change in thermodynamic conditions between the coronal hole interior and quiet-Sun regions at the base of the chromosphere.

While trying to study the nature of chromospheric oscillations at the interface between open and closed magnetic topologies, we found a quite unexpected and confounding result. We saw that at the formation heights of the *TRACE* UV continua, the plasma conditions inside a coronal hole are different from those on the coronal hole boundary and also from the quiet-Sun internetwork regions. In both cases this difference in Δz is a significant fraction of a scale height near the chromospheric temperature minimum. This result poses a challenge/question: Why would the largely hydrodynamic (high plasma-β) coronal hole interior plasma at the base of the chromosphere care about the fact that the magnetic field is open to the interplanetary medium and stratify itself so? Conventional thinking would assume that the chromosphere should have little knowledge of the topologically open coronal holes above.

Multiple equatorial and polar coronal hole regions have now been observed with the same *TRACE* Inter-Network Oscillation (INO) observing sequence in 2003 and the early part of this year; presented here is just one example. In a future paper (S. W. McIntosh et al. 2004, in preparation) we will discuss the travel-time analysis demonstrated in this Letter in detail and advance it to incorporate temporal intermittence in the chromospheric oscillations present (cf. McIntosh & Smillie 2004). In addition, we will study the other coronal hole ob-

[3] In the quiet Sun alone we can verify that the typical separation of the continuum bandpasses is of the order of 30–40 km (P. G. Judge 2004, private communication).

servations in detail and study any possible connection between the mixture of field polarities, proportion of open/closed magnetic structures, Δt and Δz in coronal hole interiors with the βTH, UV/EUV intensity/Doppler velocity contrast, and in situ solar wind measurements.

S. W. M. acknowledges the support of the Goddard Space Flight Center Solar Data Analysis Center and NASA's Living With A Star Program and would like to thank the *TRACE* team for conducting the INO program. We would like to thank Joe Gurman, Stuart Jefferies, and the anonymous referee for making many useful suggestions on the text. *SOHO* is a project of international cooperation between ESA and NASA. The *TRACE* project at Lockheed Martin is supported by NASA contract NAS5-38099. This material is based on work supported by NASA under grant NNG04GG34G issued under the Sun-Earth Connection Guest Investigator Program.

REFERENCES

Cranmer, S. R. 2002, Space Sci. Rev., 101, 229
Delaboudinière, J.-P., et al. 1995, Sol. Phys., 162, 291
Deubner, F.-L., & Fleck, B. 1990, A&A, 228, 506
Fleck, B., Domingo, V., & Poland, A. I. 1995, The *SOHO* Mission (Dordrecht: Kluwer)
Fleck, B., & McIntosh, S. W. 2003, in IAU Symp. 219, Stars as Suns: Activity, Evolution and Planets, ed. A. K. Dupree & A. O. Benz (San Francisco: ASP), 137
Handy, B. N., et al. 1999, Sol. Phys., 187, 229
Jefferies, S. M. 1998, in IAU Symp. 185, New Eyes to See inside the Sun and Stars, ed. F.-L. Deubner, J. Christensen-Dalsgaard, & D. Kurtz (San Francisco: ASP), 415
Jefferies, S. M., Osaki, Y., Shibahashi, H., Duvall, T. L., Jr., Harvey, J. W., & Pomerantz, M. A. 1994, ApJ, 434, 795
Jefferies, S. M., Osaki, Y., Shibahashi, H., Harvey, J. W., D'Silva, S., & Duvall, T. L., Jr. 1997, ApJ, 485, L49
Judge, P. G., Tarbell, T. D., & Wilhelm, K. 2001, ApJ, 554, 424
Krijger, J. M., Rutten, R. J., Lites, B. W., Straus, Th., Shine, R. A., & Tarbell, T. D. 2001, A&A, 379, 1052
McIntosh, S. W., Fleck, B., & Judge, P. G. 2003, A&A, 405, 769
McIntosh, S. W., & Judge, P. G. 2001, ApJ, 561, 420
McIntosh, S. W., & Smillie, D. G. 2004, ApJ, 604, 924
McIntosh, S. W., et al. 2001, ApJ, 548, L237
Scherrer, P. H., et al. 1995, Sol. Phys., 162, 129
Vernazza, J. E., Avrett, E. H., & Loeser, R. 1981, ApJS, 45, 635